

Original article

<https://doi.org/10.15828/2075-8545-2025-17-6-697-714>

CC BY 4.0

Experimental studies of concrete materials for the restoration of hydraulic structures

Karlygash I. Ilyassova¹ , Zhangazy N. Moldamuratov^{1,2} , Orazaly D. Seitkazinov^{1,2} ,
Guldana S. Abiyeva^{1,2*} , Ainur Z. Tukhtamisheva^{1,2*} , Manizha Paktin¹ 

¹ International Educational Corporation, Almaty, Kazakhstan

² Kazakh Leading Academy of Architecture and Civil Engineering, Almaty, Kazakhstan

* Corresponding author: e-mail: g.abieva@kazgasa.kz, aynurjan_kz@mail.ru

ABSTRACT

Introduction. The objective of this research is to substantiate the application of advanced concrete materials for restoring hydraulic structures in Kazakhstan and Central Asia, where service conditions are severe due to sharp temperature swings, sulfate-chloride attack, and high seismicity. The relevance of the study is determined by the widespread deterioration of existing infrastructure and the demonstrated inadequacy of traditional repair methods. **Methods and materials.** To evaluate the properties of the original concrete and promising repair materials (polymer-modified mortars, geopolymer systems, and ultra-high-performance concrete-UHPC), a comprehensive set of laboratory tests was conducted. The research included: physico-mechanical tests (strength, elastic modulus, adhesion), durability tests (RCPT, NT Build 492, freeze-thaw resistance, sulfate resistance, abrasion-cavitation wear), and micro/nanostructural analysis (SEM/EDS, XRD, nanoindentation). **Results and discussion.** The original concrete exhibited high permeability (~5.2 thousand C according to RCPT), low adhesion, and significant strength loss under cyclic loading, which can be explained by pronounced porosity and cracking of the structure. UHPC demonstrated minimal permeability (<0.3 thousand C), high adhesion (2.2 MPa), low strength loss under freeze-thaw cycles ($\leq 3\%$), and the highest local elastic modulus (40–50 GPa). Geopolymer materials showed strong sulfate resistance (expansion $\leq 0.038\%$) and a fine-pore structure with a low diffusion coefficient ($5 \times 10^{-12} \text{ m}^2/\text{s}$). Polymer-modified mortars (PMM) exhibited intermediate characteristics, remaining the most economically feasible option. SEM confirmed the significant densification of the UHPC and geopolymer matrices compared to the original concrete; XRD revealed a reduction in portlandite content and the formation of sulfate-resistant phases in geopolymers, while UHPC showed a predominance of amorphous C–S–H phases. **Conclusion.** The comprehensive analysis demonstrated that the rational use of materials depends on the balance between durability, reliability, and economic–environmental indicators. UHPC is recommended for zones exposed to intensive cavitation and abrasion; geopolymers are optimal for structures in sulfate environments; and PMM are suitable for localized repairs under budget constraints. The results confirm the effectiveness of a multi-level approach: diagnostics → material selection → laboratory verification → durability prediction → practical recommendations. This provides a scientifically grounded basis for designing restoration measures for hydraulic structures.







KEYWORDS: micro- and nanostructure, concrete structures, hydraulic structures, ultra-high-performance concrete (UHPC), geopolymer, polymer-modified mortars

ACKNOWLEDGMENTS: This research was carried out with the financial support of the Science Committee of the Ministry of Science and Higher Education of the Republic of Kazakhstan under the scientific project No. AP23487624.

FOR CITATION:

Ilyassova K.I., Moldamuratov Zh.N., Seitkazinov O.D., Abiyeva G.S., Tukhtamisheva A.Z., Paktin M. Experimental studies of concrete materials for the restoration of hydraulic structures. *Nanotechnologies in construction*. 2025;17(6):697–714. <https://doi.org/10.15828/2075-8545-2025-17-6-697-714>. – EDN: OBIJOJ.

Экспериментальные исследования бетонных материалов для восстановления конструкций гидротехнических сооружений

Карлыгаш Идрисовна Ильясова¹ , Жангазы Нуржанович Молдамуратов^{1,2} ,
Оразалы Дауткалиевич Сейтказинов^{1,2} , Гулдана Солтановна Абиева^{1,2*} ,
Айнур Зокировна Тухтамишева^{1,2*} , Манижа Пактин¹ 

¹ Международная образовательная корпорация, Алматы, Казахстан

² Казахская головная архитектурно-строительная академия, Алматы, Казахстан

* Автор, ответственный за переписку: e-mail: g.abieva@kazgasa.kz, aynurjan_kz@mail.ru

АННОТАЦИЯ

Введение. Целью исследования являлось обоснование применения современных бетонных материалов для восстановления конструкций гидротехнических сооружений в условиях Казахстана и Центральной Азии, где эксплуатация осложнена резкими климатическими перепадами, сульфатно-хлоридной агрессией и сейсмической активностью. Актуальность работы определяется высокой степенью износа действующих сооружений и недостаточной эффективностью традиционных методов ремонта. **Методы и материалы.** Для оценки свойств исходного бетона и перспективных ремонтных составов (полимермодифицированные растворы, геополимерные системы и ультравысокопрочный бетон – УНПС) проведен комплекс лабораторных испытаний. Исследования включали физико-механические тесты (прочность, модуль упругости, адгезия), долговечностные испытания (RCPT, NT Build 492, морозостойкость, сульфатная стойкость, абразивно-кавиционный износ) и анализ микро- и наноструктуры (SEM/EDS, XRD, наноиндентация). **Результаты и обсуждение.** Исходный бетон показал высокую проницаемость (~5,2 тыс. Кл по RCPT), низкую адгезию и значительные потери прочности при циклировании, что объясняется выраженной пористостью и трещиноватостью структуры. УНПС продемонстрировал минимальную проницаемость (<0,3 тыс. Кл), высокую адгезию (2,2 МПа), низкие потери прочности при морозных циклах ($\leq 3\%$) и максимальные значения локального модуля упругости (40–50 ГПа). Геополимерные материалы обеспечили стойкость к сульфатной агрессии (расширение $\leq 0,038\%$) и мелкопористую структуру с низким коэффициентом диффузии ($5 \times 10^{-12} \text{ м}^2/\text{с}$), полимермодифицированные растворы (ПММ) показали промежуточные характеристики, оставаясь экономически более доступным решением. SEM подтвердил значительное уплотнение структуры УНПС и геополимеров по сравнению с исходным бетоном; XRD выявил снижение содержания портландита и образование сульфатостойких фаз у геополимеров, а у УНПС – преобладание аморфного C–S–H. **Заключение.** Комплексный анализ показал, что рациональность применения материалов определяется сочетанием эксплуатационной долговечности, надежности и экономико-экологических показателей. УНПС следует рекомендовать для зон с интенсивной кавитацией и абразией, геополимеры – для сооружений в сульфатных средах, а ПММ – для локальных ремонтных работ в условиях ограниченного бюджета. Результаты исследования подтверждают эффективность многоуровневого подхода: диагностика → выбор материала → лабораторная верификация → прогноз долговечности → практические рекомендации. Это обеспечивает научно обоснованную основу для проектирования восстановительных мероприятий гидротехнических сооружений.

КЛЮЧЕВЫЕ СЛОВА: микро- и наноструктура, бетонные конструкции, гидротехнические сооружения, ультравысокопрочный бетон, геополимер, полимермодифицированные растворы

БЛАГОДАРНОСТИ: Исследование выполнено при финансовой поддержке Комитета науки Министерства науки и высшего образования Республики Казахстан в рамках научного проекта № AP23487624.

ДЛЯ ЦИТИРОВАНИЯ:

Ильясова К.И., Молдамуратов Ж.Н., Сейтказинов О.Д., Абиева Г.С., Тухтамишева А.З., Пактин М. Экспериментальные исследования бетонных материалов для восстановления конструкций гидротехнических сооружений. *Нанотехнологии в строительстве*. 2025;17(6):697–714. <https://doi.org/10.15828/2075-8545-2025-17-6-697-714>. – EDN: OBIJOJ.

INTRODUCTION

Concrete hydraulic structures (HS) are the foundation of sustainable water management. They ensure river flow regulation, irrigation, urban water supply, electricity generation, and flood protection [1, 4, 5]. The reliability and

durability of these structures directly influence the socio-economic development of nations. In Kazakhstan and other Central Asian countries, most concrete hydraulic structures were built between the 1960s and 1980s, with a designed service life of 40–50 years. Today, a significant portion of these facilities have exceeded their normative

operational lifespan. According to the Ministry of Ecology and Water Resources of the Republic of Kazakhstan, more than 60% of hydraulic facilities require repair or reconstruction. In Uzbekistan and Kyrgyzstan, similar figures range between 55–65% [2, 3, 6, 7].

In Central Asia, the operation of concrete hydraulic structures is complicated by a combination of natural and anthropogenic factors. Sharp temperature fluctuations, repeated freeze–thaw cycles, and intense solar radiation accelerate concrete degradation. Saline groundwater in the Aral Sea basin and the lower reaches of the Syrdarya River cause chloride and sulfate corrosion, leading to the loss of protective properties of both concrete and reinforcement. In the seismically active regions of Kazakhstan, Kyrgyzstan, and Tajikistan, dynamic loads promote crack formation and reduce the bond strength between concrete and reinforcement. Aging canals and spillways operate under overload conditions due to population growth and agricultural demands. Traditional repair methods, such as cement injections and shotcrete, provide only short-term effects. Limited funding further constrains the adoption of durable rehabilitation technologies [1–4, 10, 11].

International experience identifies six key deterioration mechanisms of concrete hydraulic structures: carbonation and loss of concrete protective capacity; rebar corrosion caused by chlorides; sulfate attack in mineralized waters; cavitation and abrasion in high-head spillways; frost damage in continental climates; and the alkali–silica reaction typical of concretes with local aggregates (Table 1).

In Central Asia, these are compounded by seismic risks, high water salinity, and large fluctuations in reservoir levels.

Currently, researchers worldwide [13–18] are investigating new materials and approaches—ultra-high-performance concrete (UHPC), polymer-modified mortars, geopolymer systems, cathodic protection, and digital monitoring methods. However, their implementation in

the region remains limited due to the lack of scientifically grounded methodologies and adaptation to local conditions [19, 20].

Global practice has accumulated significant experience in the rehabilitation of concrete hydraulic structures, aimed at extending service life, reducing failure risks, and enhancing resistance to aggressive environmental impacts. Modern approaches are based on the integration of engineering technologies, innovative materials, and digital monitoring systems [12, 21, 22].

The diagnosis of defects is actively advancing through the use of non-destructive testing methods such as ultrasonic testing, ground-penetrating radar (GPR), infrared thermography, and acoustic emission analysis. Unmanned aerial vehicles equipped with LiDAR systems have become widely used, as have digital twins and BIM models that integrate monitoring results into a unified information environment. In the United States and the European Union, sensor-based systems are being implemented to monitor moisture levels, reinforcement corrosion, and crack propagation [23, 24].

Restoration methods include shotcreting to reinforce canal and spillway linings; injection technologies using epoxy resins, polyurethanes, and microcements for crack sealing; lining with high-strength concrete (UHPC, RCC); and the use of polymer membranes and composites. Structural strengthening is carried out using FRP systems, carbon and glass fiber materials, and textile-reinforced matrices (TRM). To protect reinforcement, cathodic protection and electrochemical chloride removal techniques are applied. Geopolymer materials and secondary mineral additives (fly ash, steelmaking slags) are increasingly used, providing both environmental benefits and enhanced resistance to sulfate attack (Table 2) [25, 26].

Practical examples confirm the effectiveness of these technologies. In Norway and Canada, geopolymer mor-

Table 1. Common Defects Observed in Concrete Hydraulic Structures throughout Central Asia

No.	Defect	Cause	Regional Characteristics	Consequences
1	Carbonation	CO ₂ diffusion	High solar radiation, arid climate	Loss of protective layer
2	Chloride corrosion	Saline water	Aral Sea region, lower Syr Darya basin	Reinforcement corrosion
3	Sulfate corrosion	Mineralized water	Southern Kazakhstan, Fergana Valley	Formation of ettringite, cracking
4	Frost damage	Freeze–thaw cycles	Northern and Eastern Kazakhstan	Concrete scaling and spalling
5	Cavitation and abrasion	High flow velocity	Conduits and spillways of Charyn and Shardara HPPs	Pitting, surface erosion
6	Seismic cracking	Dynamic loads	Almaty, Bishkek, Dushanbe	Loss of structural integrity

Table 2. International Technologies for the Rehabilitation of Concrete Hydraulic Structures

No.	Technology	Application	Advantages	Disadvantages
1	Shotcrete	Canal and dam lining	Fast application, cost-effective	Short service life (10–15 years)
2	Injections (epoxy, PU, microcement)	Cracks and joints	Restores watertightness	Difficult quality control
3	UHPC, RCC	Lining and facing	High durability (>50 years)	High cost
4	FRP, TRM	Structural strengthening	Lightweight, corrosion-resistant	Limited experience in hydraulic structures
5	Geopolymers	Cement replacement	Eco-friendly, sulfate-resistant	Limited regulatory framework
6	Cathodic protection	Reinforcement protection	Effective up to 30 years	Expensive and maintenance-intensive

tars with low heat of hydration are used for dam rehabilitation, reducing the risk of thermal cracking. In China and Japan, ultra-high-performance concretes are widely applied for spillway and canal lining, ensuring service lives exceeding 50 years. In the United States, the U.S. Army Corps of Engineers employs cathodic protection and electrochemical desalination systems, extending the service life of structures by 20–30 years. In EU countries, a multi-level “diagnosis–repair–monitoring” approach is implemented, within which digital twins of structures are updated in real time (Fig. 1) [27, 28].

The main trends in international practice include the shift from local repairs to comprehensive rehabilitation, the implementation of environmentally sustainable materials and technologies considering life-cycle indicators, the active use of digital tools for monitoring and residual service life prediction, and the multi-criteria optimization of solutions based on the “cost–reliability–environment” approach [25–30].

Global experience shows that long-term durability of repairs is achieved through the integration of modern materials, innovative technologies, and digital monitoring.

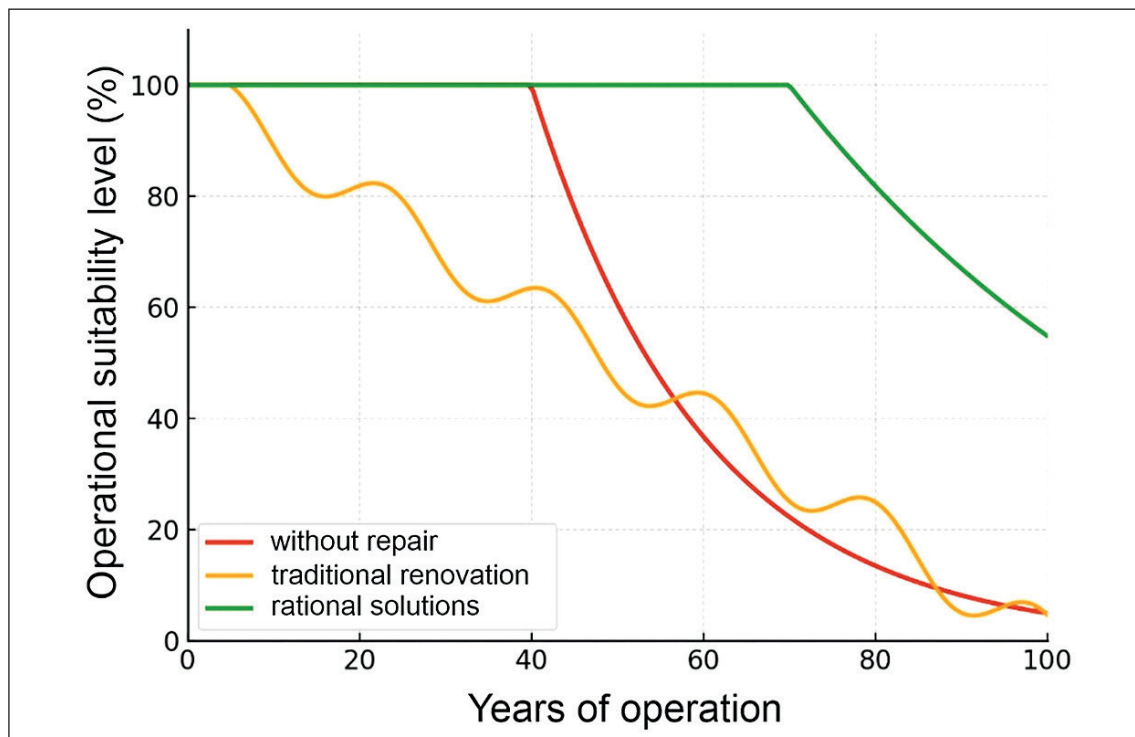


Fig. 1. Life cycle of concrete hydraulic structures

For Central Asia, the key challenge is the adaptation of these practices considering the region’s climatic, seismic, and hydrogeological conditions [26–29].

The main scientific problem lies in the absence of a systematic approach to justifying rational technical solutions that account for defect characteristics, climatic factors, economic constraints, and durability requirements.

The purpose of the study is to substantiate rational technical solutions for restoring the operational performance of concrete structures in hydraulic facilities of Kazakhstan and Central Asia.

Research objectives:

- systematize defects and factors of their occurrence under regional conditions;
- develop a comprehensive diagnostic methodology for concrete hydraulic structures;
- investigate the properties of modern repair materials in the aggressive environments of Central Asia;
- model the behavior of structures considering climatic and seismic factors;
- perform a multifactor assessment of solution rationality according to the criteria of durability, reliability, economy, and ecology;
- formulate recommendations for practical application in the repair and reconstruction of hydraulic structures.

MATERIALS AND METHODS

1. Materials and specimen series [13–22].

Four material systems representing practical repair solutions for hydraulic structures were studied: control cores, polymer-modified mortar (PMM), ultra-high-performance concrete (UHPC), and a geopolymer composition (GP). The mixed designs and target characteristics are summarized in Table 3.

Specimens were cast in cylinders Ø100×200 mm and cubes 100×100×100 mm; prisms 100×100×400 mm were used for modulus testing. The curing regime was 28 days at 20±2 °C and RH ≥ 95%. Before testing, specimen ends were ground or capped.

2. Conditioning [26].

Preparation regimes for specific test methods are presented in Table 5. For NT Build 492, vacuum saturation (50 kPa, 1 h) followed by 24 h water immersion at 23 °C was used. RCPT specimens were saturated according to ASTM C1202 (24 h). For sorptivity testing (ASTM C1585), samples were oven-dried at 50 °C until mass stabilization, then subjected to one-sided capillary absorption. Freeze–thaw resistance was tested under regimes A/B (–18 ... +4 °C) up to 300 cycles; sulfate resistance was evaluated in Na₂SO₄/MgSO₄ solutions (50 g/L) at 23 °C for 6–12 months. A simplified schedule for the first 120 days is shown in Figure 2.

3. Physical and mechanical tests [17, 21, 27].

Compressive strength was determined according to ASTM C39/EN 12390-3 on Ø100×200 mm cylinders and cores; the modulus of elasticity was measured according to ASTM C469/EN 12390-13 on prisms using strain gauges. Water absorption (ASTM C642) and capillary sorptivity (ASTM C1585) were used to assess transport properties; the target value for repair compositions was $k_{sorp} \leq 0.10 \text{ kg/m}^2 \cdot \text{h}^{0.5}$. The planned number of specimens for each test type is shown in Figure 3.

4. Permeability and migration [13–15].

Ion permeability was evaluated using the Rapid Chloride Permeability Test (RCPT, ASTM C1202, 6 h, 60 V; target < 1000 °C), while diffusion characteristics were measured by the migration test NT Build 492, calculating $D_{nssm} \leq 8 \times 10^{-12} \text{ m}^2/\text{s}$ for the best systems. Discs Ø100×50 mm was prepared from the same mixtures as the mechanical specimens, with identical curing and pre-saturation conditions.

5. Durability exposures [17, 21].

Freeze–thaw resistance was tested per ASTM C666 (regimes A/B) and CDF (RILEM), monitoring changes in mass, dynamic modulus, and residual strength after 56–300 cycles. Sulfate resistance was assessed according to ASTM C1012 in 50 g/L Na₂SO₄/MgSO₄ solutions by measuring expansion deformations. Abrasion resistance was determined by ASTM C1138 (up to 12 h), and cavita-

Table 3. Mix compositions and target characteristics of the systems

No.	System	Binder	Aggregate / Fraction	d_{max}' / mm	w/b or M_s	Polymer p/c, %	Fiber, % vol.	Additives	Target f_c , MPa	Modulus E, GPa	Notes
1	Control cores	Portland cement (from structure)	Crushed stone / sand, up to 20 mm	20	–	–	–	–	30–40 (actual)	25–32	Baseline
2	PMM mortar	Portland cement + polymer dispersion	Quartz sand 0–2 mm	2	w/c = 0.35	7	0	SP 0.6–1.0%	40–80	25–35	Low shrinkage
3	UHPC	PC + microsilica + fly ash / slag	Quartz flour + sand 0–1 mm	1	w/b = 0.18–0.20	–	2 (steel)	SP 1.0–1.5%	≥150	40–50	High wear resistance
4	Geopolymer (GP)	Fly ash + BOFS, alkaline activator	Sand 0–2 mm	2	$M_s = 1.4$; LA = 10%	–	0–0.5 (opt.)	Plasticizer 0.5–0.8%	60–90	28–38	Sulfate resistance

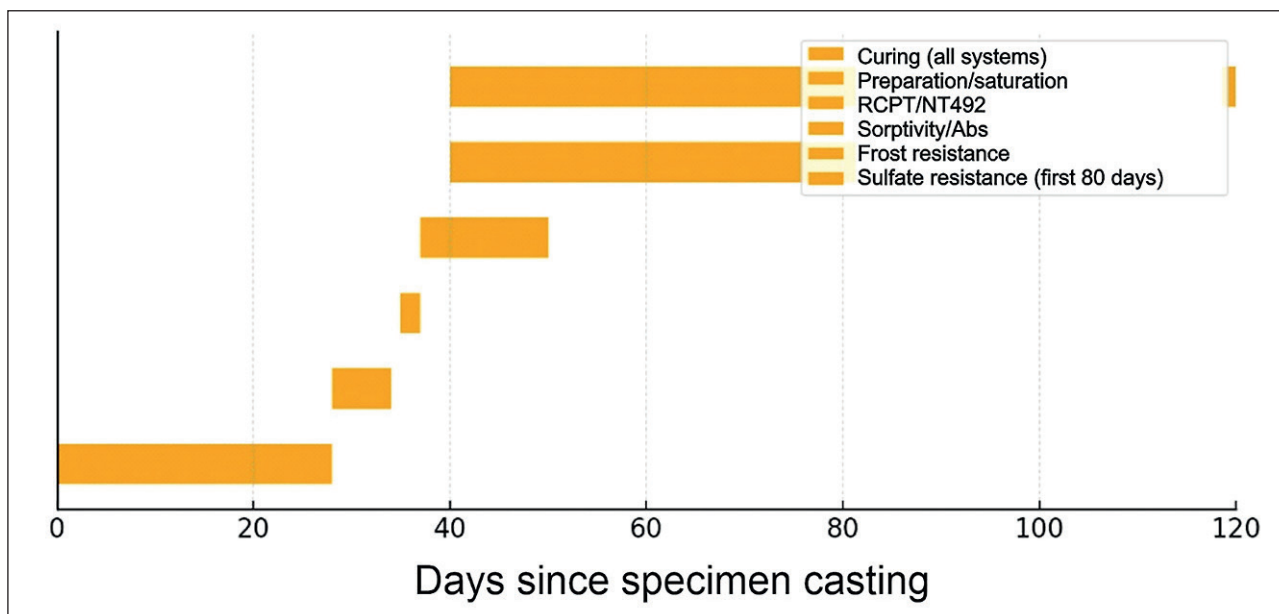


Fig. 2. Conditioning and testing schedule (first 120 days)

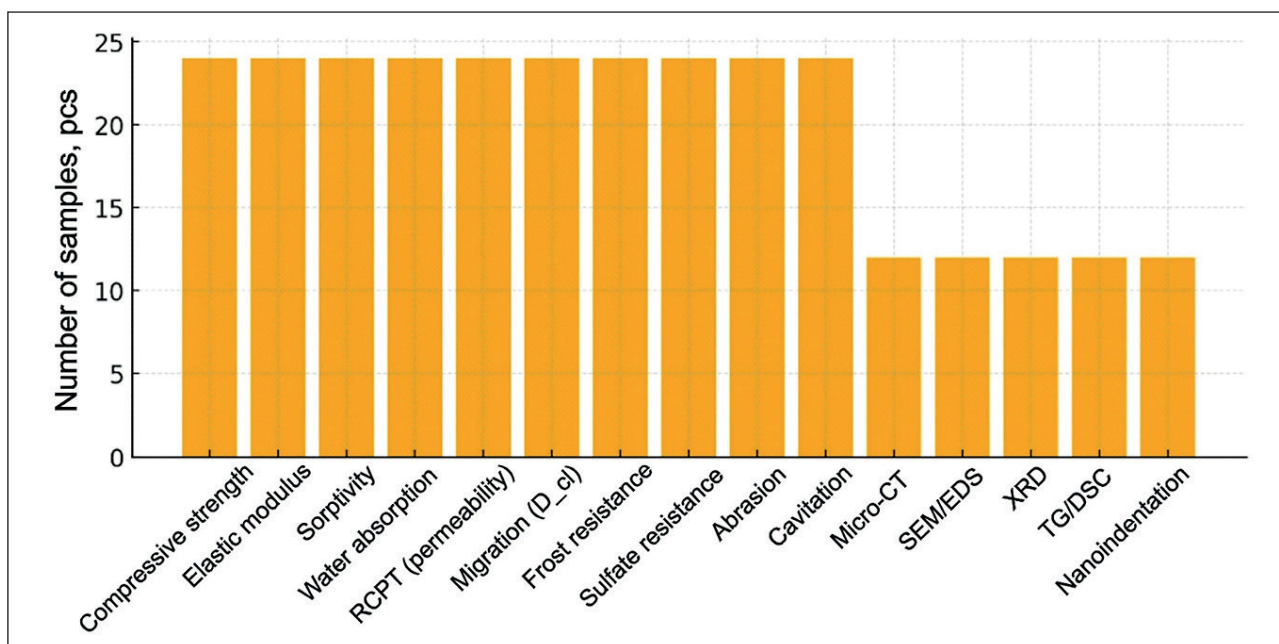


Fig. 3. Specimen quantity plan by test type

tion erosion by ASTM G32 (vibratory method), recording the specific wear rate.

6. Micro- and nanostructure [1, 4, 5].

SEM/EDS (15–20 kV) was used for mapping the interfacial transition zone (ITZ), microcracks, and Cl⁻/S distribution in coating and substrate areas. XRD (CuK α , 2 θ = 5–70°, step 0.02°) enabled quantitative phase identification (portlandite, ettringite, carbonates, Friedel’s salt). TG/DSC (10 °C/min up to 1000 °C) was employed to evaluate C–S–H dehydration, CH dehydroxylation,

and decarbonation. Mercury intrusion porosimetry (MIP, 0.003–300 μ m) provided pore size distribution and total porosity. Micro-CT (10–30 μ m/voxel) was used to quantify 3D porosity, connectivity, and microcrack density. Nanoindentation (ISO 14577, grid 10 \times 10, step 5–10 μ m) was applied to determine local E and H of C–S–H (LD/HD) and ITZ regions.

7. Test volumes and standards [22–22].

The complete test matrix, standards, specimen types, and testing volumes for each system are presented

in Table 4. For mechanical and transport tests, at least $n = 6$ specimens per system were used; for microstructural methods – $n = 3$ thin sections/samples per system. Repeatability was controlled by duplicate tests ($\geq 10\%$) and reference samples (XRD, TG/DSC).

RESULTS AND DISCUSSION

Compressive Strength and Elastic Modulus

The tests revealed a significant difference between the systems studied (Fig. 4). The control cores exhibited an average compressive strength of 34 MPa and an elastic modulus of approximately 27 GPa. The polymer-modified mortars (PMM) reached 58 MPa and 31 GPa. Geopolymer samples achieved 72 MPa and 34 GPa. UHPC exceeded 150 MPa with a modulus of around 47 GPa. Thus, UHPC demonstrates more than a fourfold increase in strength compared to the original concrete, while geopolymer compositions show a stable improvement, particularly in terms of modulus.

Transport Properties (RCPT, Migration, Sorptivity)

According to the RCPT (ASTM C1202) results, the charge for the original samples was approximately 5000 °C, indicating high permeability. For PMM, this value decreased to 1500 °C; for geopolymers, to 800 °C;

and for UHPC, to less than 300 °C (Fig. 5). The migration coefficient (NT Build 492) confirmed the same trend: a one-order-of-magnitude reduction for UHPC and a sixfold reduction for geopolymers. Sorptivity tests showed minimal capillary water absorption for UHPC ($\sim 0.03 \text{ kg/m}^2 \cdot \text{h}^{0.5}$), while the original samples exhibited $0.25 \text{ kg/m}^2 \cdot \text{h}^{0.5}$.

Durability: Freeze–Thaw, Sulfate, Cavitation, and Abrasion

Freeze–thaw resistance (ASTM C666) confirmed severe degradation of the original concrete, with strength loss reaching 22% after 300 cycles. UHPC showed only a 3% loss, geopolymer materials 5%, and PMM 8%. In the sulfate environment (ASTM C1012), the maximum expansion reached 0.30% for the original concrete compared to 0.04% for geopolymers and 0.06% for UHPC. Thus, geopolymers demonstrated the highest sulfate resistance. Abrasion and cavitation wear tests revealed that UHPC had the lowest wear rate – mass loss was 6–7 times lower compared to the original concrete (Fig. 6 and 7).

Microstructure and Nanostructure

SEM images revealed pronounced pores and cracks in the original concrete, a denser structure in PMM, a more

Table 4. Test program and applicable standards

No.	Test	Standard / Reference	Specimen Type / Size	n per system	Output Parameter
1	Compressive strength	ASTM C39 / EN 12390-3	Cylinder $\varnothing 100 \times 200$ mm	6	f_c (MPa)
2	Elastic modulus	ASTM C469 / EN 12390-13	Prism $100 \times 100 \times 400$ mm	6	E (GPa)
3	Sorptivity	ASTM C1585	Disk / cube (one-side saturation)	6	k_{sorp} ($\text{kg/m}^2 \cdot \text{h}^{0.5}$)
4	Water absorption	ASTM C642	Cube $100 \times 100 \times 100$ mm	6	A_{bs} (%)
5	RCPT (permeability)	ASTM C1202	Disk $\varnothing 100 \times 50$ mm	6	Charge (C)
6	Migration (Dcl)	NT Build 492	Disk $\varnothing 100 \times 50$ mm	6	D_{nssm} (m^2/s)
7	Freeze–thaw resistance	ASTM C666 / CDF RILEM	Prism / cube	6	$\Delta m, \Delta E_{dyn}, \Delta f_c$
8	Sulfate resistance	ASTM C1012	Prism specimen	6	Expansion (%)
9	Abrasion	ASTM C1138	Plate / cube	6	Mass loss ($\text{g/m}^2 \cdot \text{h}$)
10	Cavitation	ASTM G32	Plate / cube	6	Wear (mg/min)
11	Micro-CT	Internal protocol	Cube / core	3	Porosity, connectivity, cracking
12	SEM/EDS	Internal protocol	Polished section	3	ITZ, Ca/Si, Cl, S distribution
13	XRD	Internal protocol	Powder	3	Phase composition
14.	TG/DSC	Internal protocol	Powder	3	CH, carbonates, hydrates
15	Nanoindentation	ISO 14577 (procedure)	Polished section	3	Local E, H

Table 5. Conditioning and specimen preparation

No.	Stage	Regime	Duration	Specimens
1	Curing	20±2 °C; RH ≥ 95%	28 days	All systems
2	End preparation	Grinding / capping	Before testing	Compression, modulus
3	Vacuum saturation	50 kPa, 1 h; conditioning at 23 °C, 24 h	Before NT492	Discs Ø100×50 mm
4	RCPT conditioning	Saturation per ASTM C1202	24 h	Discs Ø100×50 mm
5	Sorptivity	Drying at 50 °C to m _{stab} → end-face saturation	per ASTM C1585	Discs / cubes
6	Freeze–thaw	Regime A/B; –18...+4 °C	up to 300 cycles	Prisms / cubes
7	Sulfate exposure	Na ₂ SO ₄ / MgSO ₄ , 50 g/L, 23 °C	6–12 months	Prisms
8	Micro-CT	No impregnation; orientation fixed	–	Cores / cubes
9	SEM/EDS	Epoxy impregnation; Au/Pd coating	–	Polished sections
10	Nanoindentation	Polishing to 1 µm; 23 °C, 50% RH	–	Polished sections

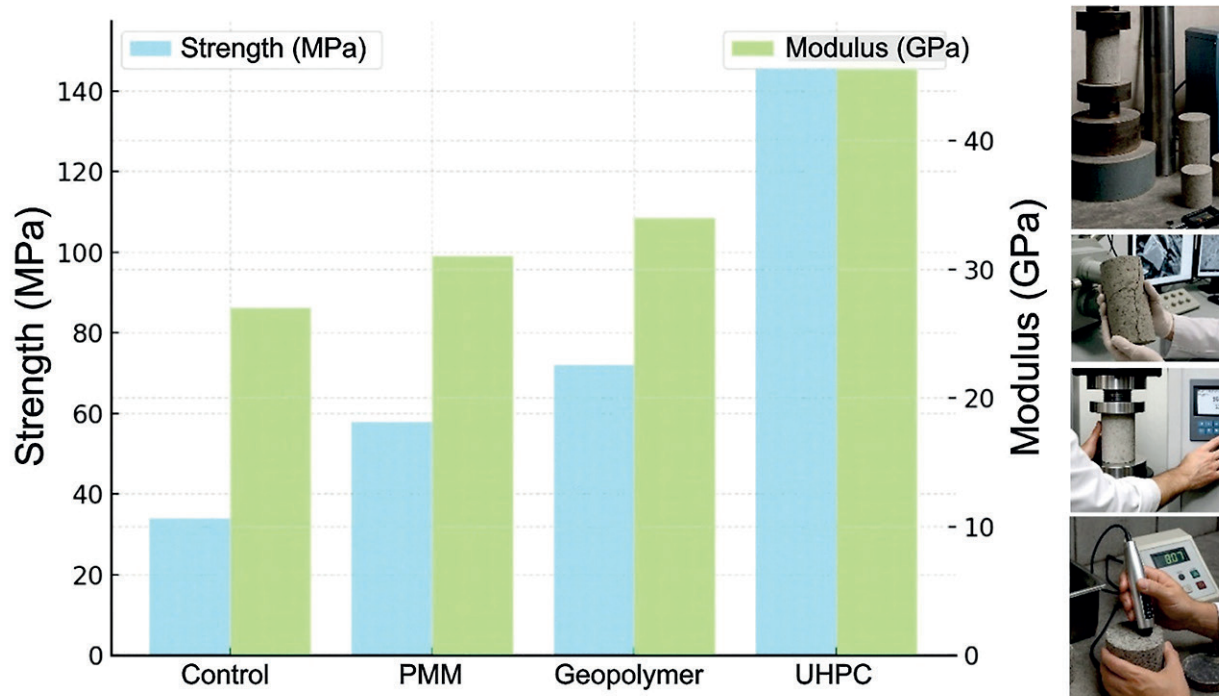


Fig. 4. Compressive strength and elastic modulus of the systems

uniform and fine-pored matrix in geopolymers, and an extremely compact matrix in UHPC with evenly distributed steel fibers (Fig. 8).

In the original concrete, SEM images at magnifications of 1000×, 5000×, and 20,000× clearly showed high porosity and numerous cracks, indicating low homogeneity of the cement matrix. At 1000× magnifica-

tion, large spherical pores and weak interfacial bonding defects were visible; at 5000×, the structure appeared granular, with uneven particle distribution and a poorly formed matrix. At 20,000×, loose aggregates of hydration products and poorly connected C–S–H gel were observed, indicating limited durability of the original material (Fig. 8a).

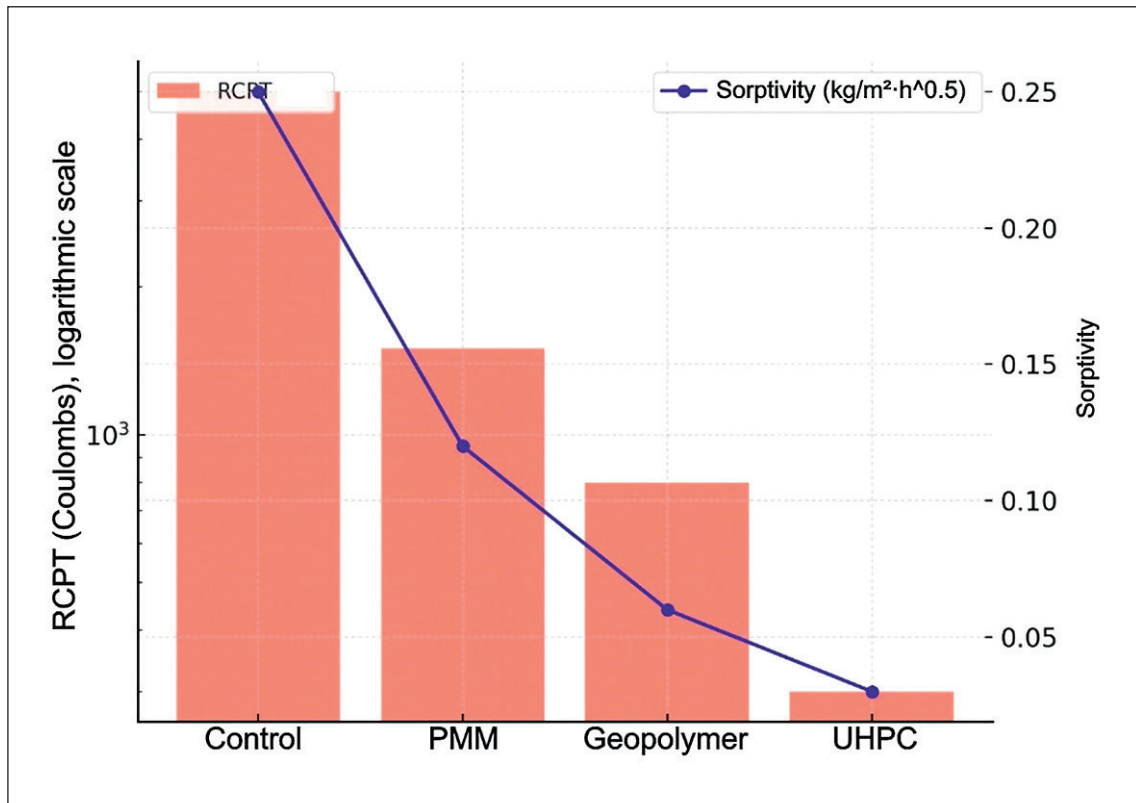


Fig. 5. Transport properties: RCPT and sorptivity

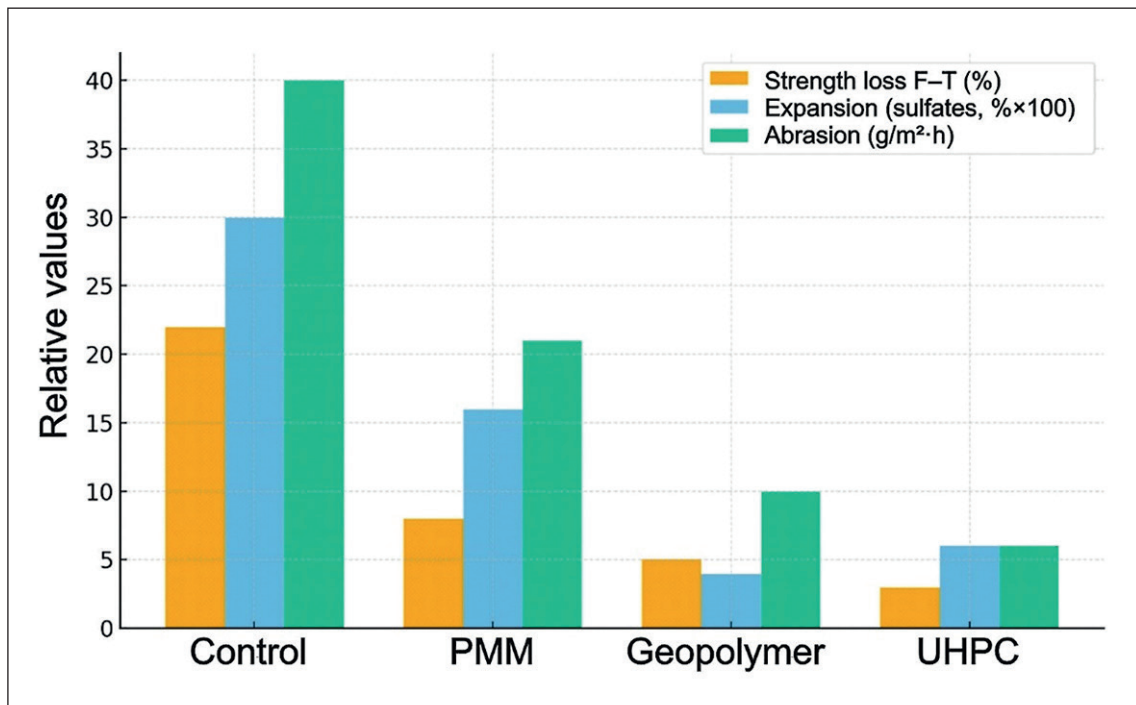


Fig. 6. Durability performance indicators

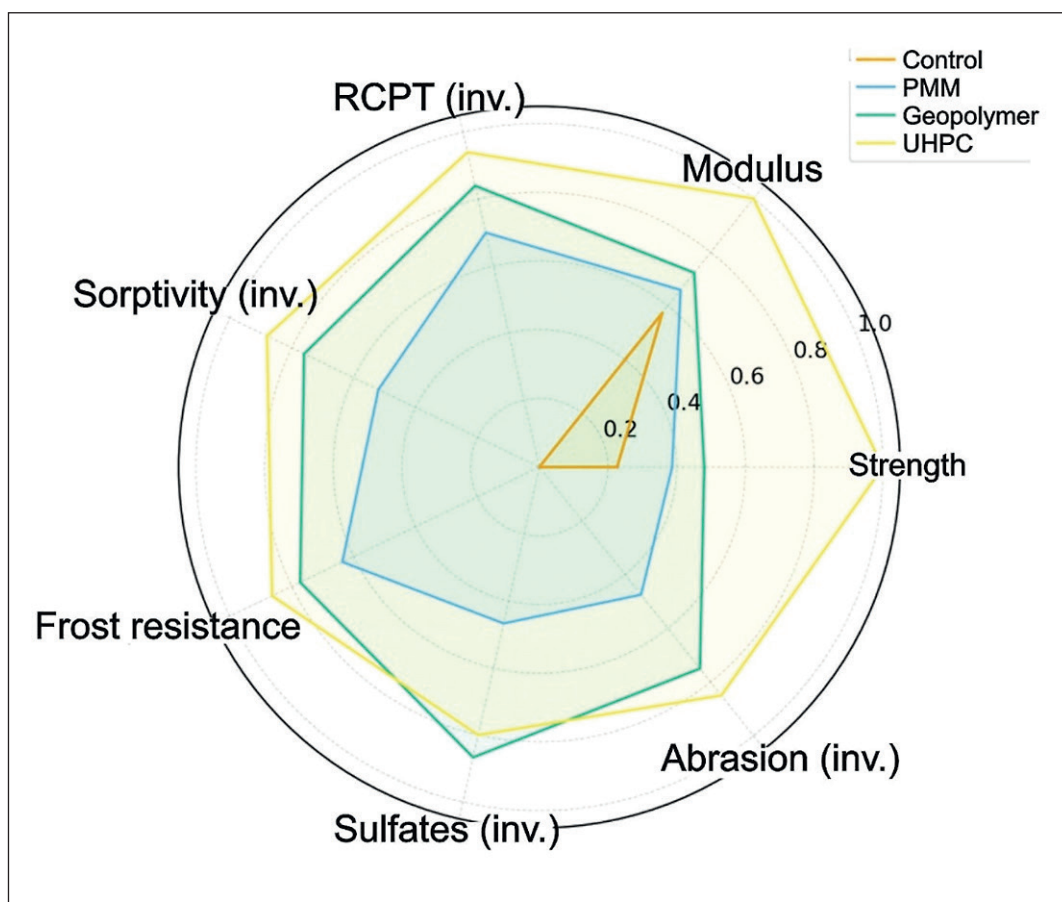


Fig. 7. Comprehensive evaluation of material properties

The polymer-modified mortar (PMM) exhibited a denser structure. At 1000 \times , a uniform matrix with fewer macropores was evident. At 5000 \times , the surface appeared compact with small pores and smoothed particle boundaries due to the polymer phase. At 20,000 \times , the structure was represented by a homogeneous amorphous matrix with nanopores, explaining the improved watertightness and strength of PMM compared to the original concrete (Fig. 8b).

The geopolymer composition was characterized by a fine-pored, homogeneous structure. At 1000 \times magnification, no large cracks were detected, and the pore distribution was uniform. At 5000 \times , the matrix appeared denser, with zones of newly formed phases—hydrosulfoaluminates—replacing portlandite. At 20,000 \times , the structure consisted of a dense amorphous nanogel (C–A–S–H), which ensures high sulfate resistance and long-term durability of the material (Fig. 8c).

Ultra-high-performance concrete (UHPC) showed the most compact and uniform structure among all systems. At 1000 \times , minimal porosity and uniform distribution of steel fibers within the matrix were observed. At 5000 \times , the cement matrix was almost fully densified, with no macropores. At 20,000 \times , an amorphous C–S–H

gel with a homogeneous nanostructure and minimal secondary phases was identified, providing UHPC with exceptional mechanical performance, including a local elastic modulus of 40–50 GPa (Fig. 8d).

XRD analysis revealed that the geopolymer samples exhibited a marked reduction in portlandite content and the formation of hydrosulfoaluminate phases, which enhance sulfate resistance. UHPC, in turn, showed a minimal presence of secondary crystalline phases and a dominant amorphous C–S–H component (Fig. 9).

In the original concrete, the diffractogram clearly displayed intense portlandite peaks at $2\theta \approx 18^\circ$, along with quartz reflections at 27° , 34° , and 47° . The high intensity of the portlandite peak indicates a significant amount of free $\text{Ca}(\text{OH})_2$, making the material vulnerable to sulfate and carbonation corrosion. The crystalline index was high, with almost no amorphous phase present, confirming the dominance of crystalline components. Calculations using the Scherrer equation showed that the average crystallite size of portlandite was about 50–60 nm (Fig. 10).

The polymer-modified mortar (PMM) demonstrated a reduction in the intensity of the portlandite peak around 18° , indicating more complete hydration and binding of

free $\text{Ca}(\text{OH})_2$. The quartz peaks at 27° , 34° , and 47° remained visible, though the background of the diffractogram appeared smoother. The crystallinity index was lower than that of the original concrete, associated with the formation of amorphous hydration phases. The aver-

age portlandite crystallite size decreased to 35–40 nm, correlating with matrix densification and reduced porosity in PMM (Fig. 11).

In the geopolymer composition, portlandite content decreased significantly, while new phase peaks appeared

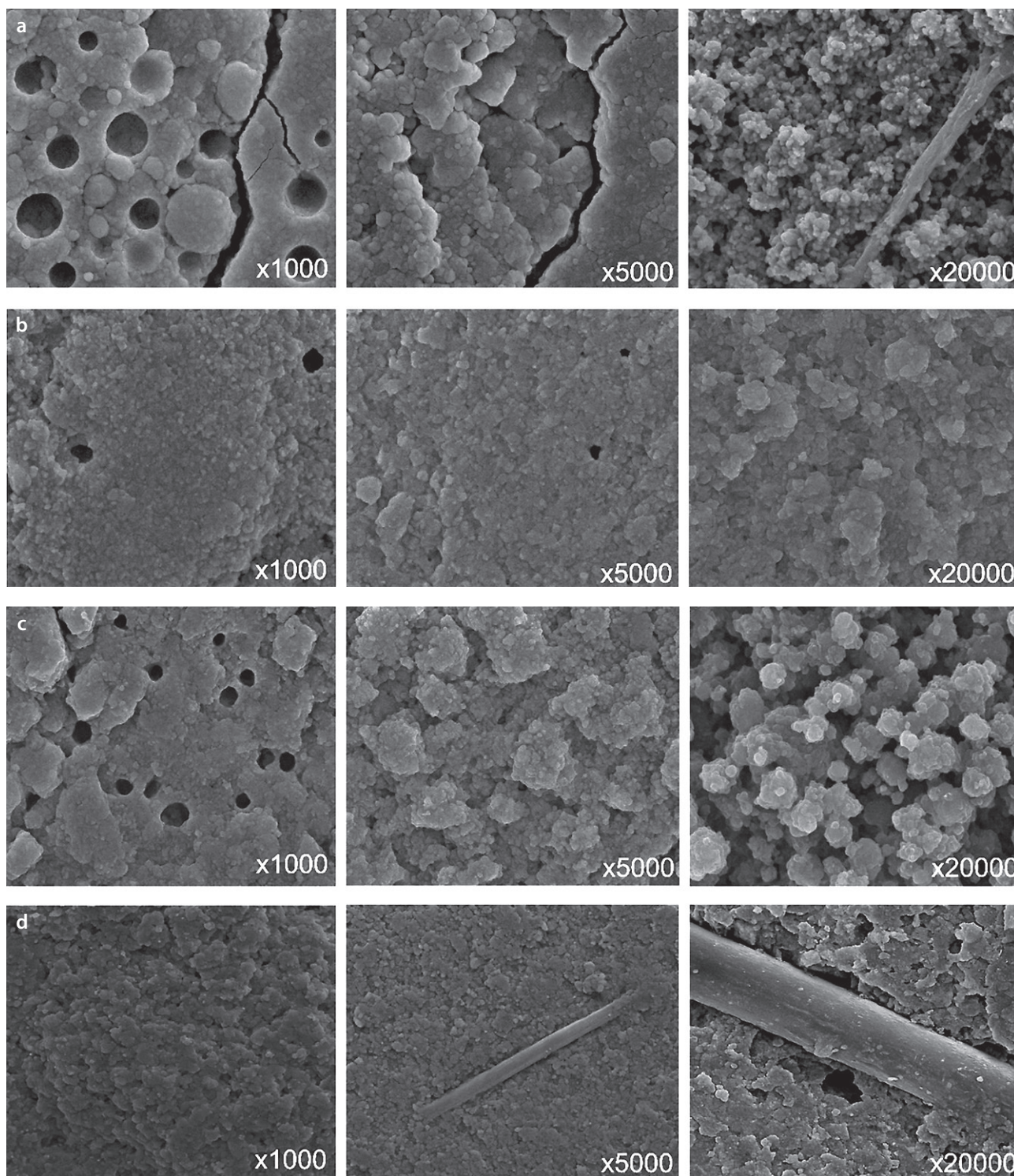


Fig. 8. SEM images: (a) original concrete; (b) PMM; (c) GP; (d) UHPC

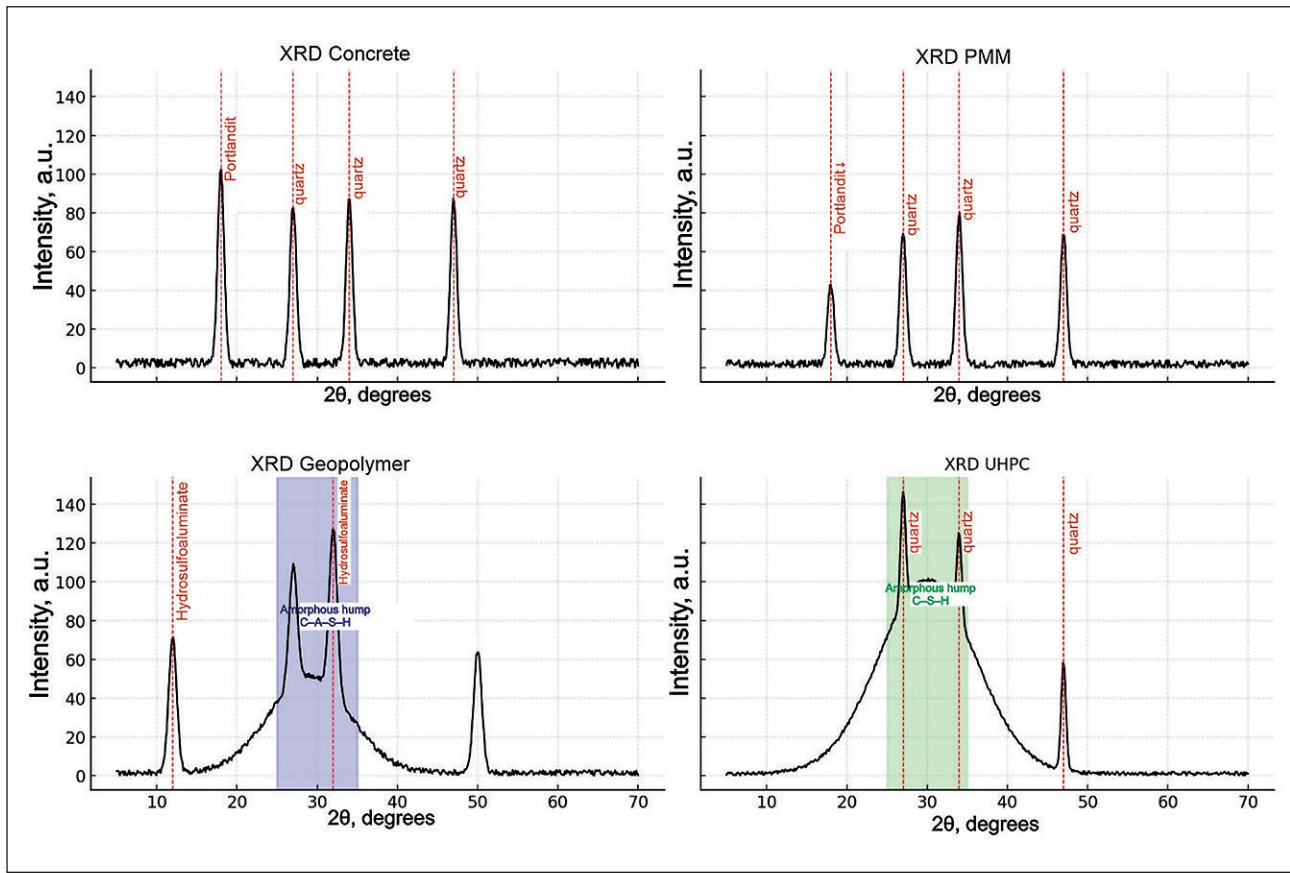


Fig. 9. X-ray diffraction (XRD) analysis highlighting amorphous phases

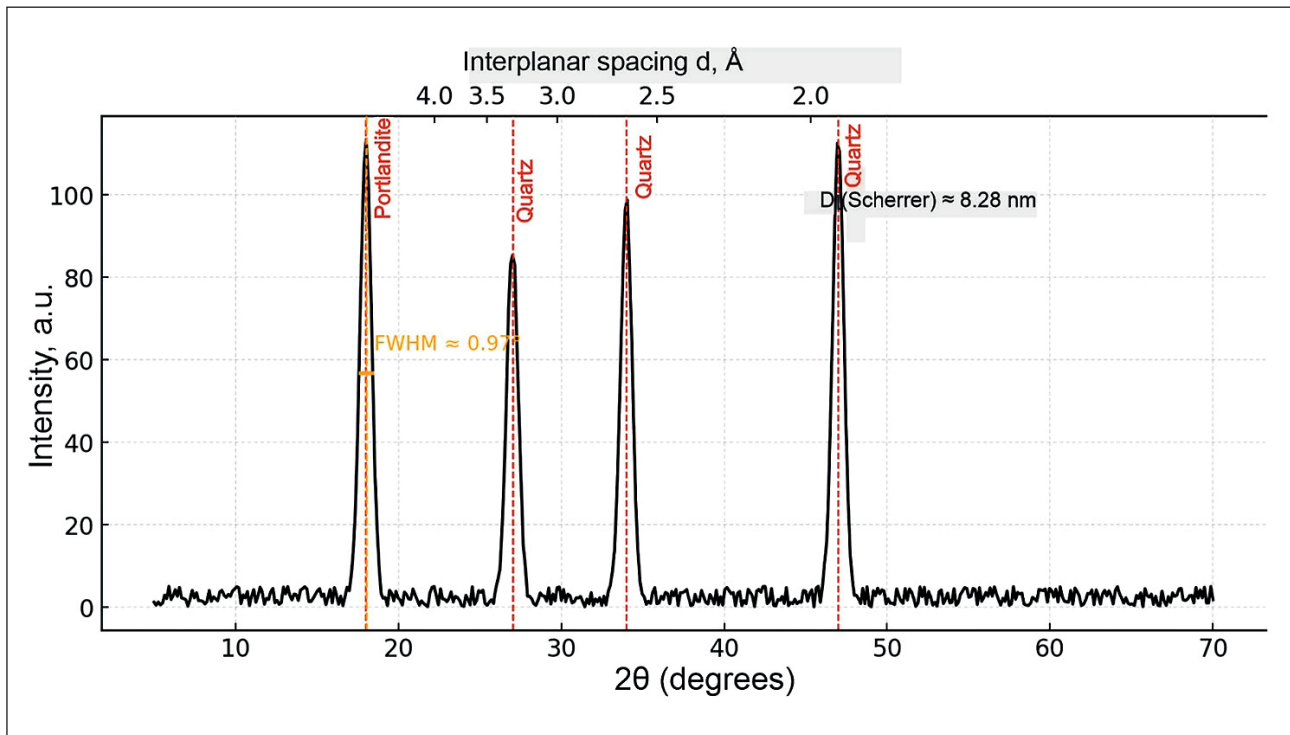


Fig. 10. X-ray diffraction (XRD) of original concrete: peaks, FWHM, d-axis

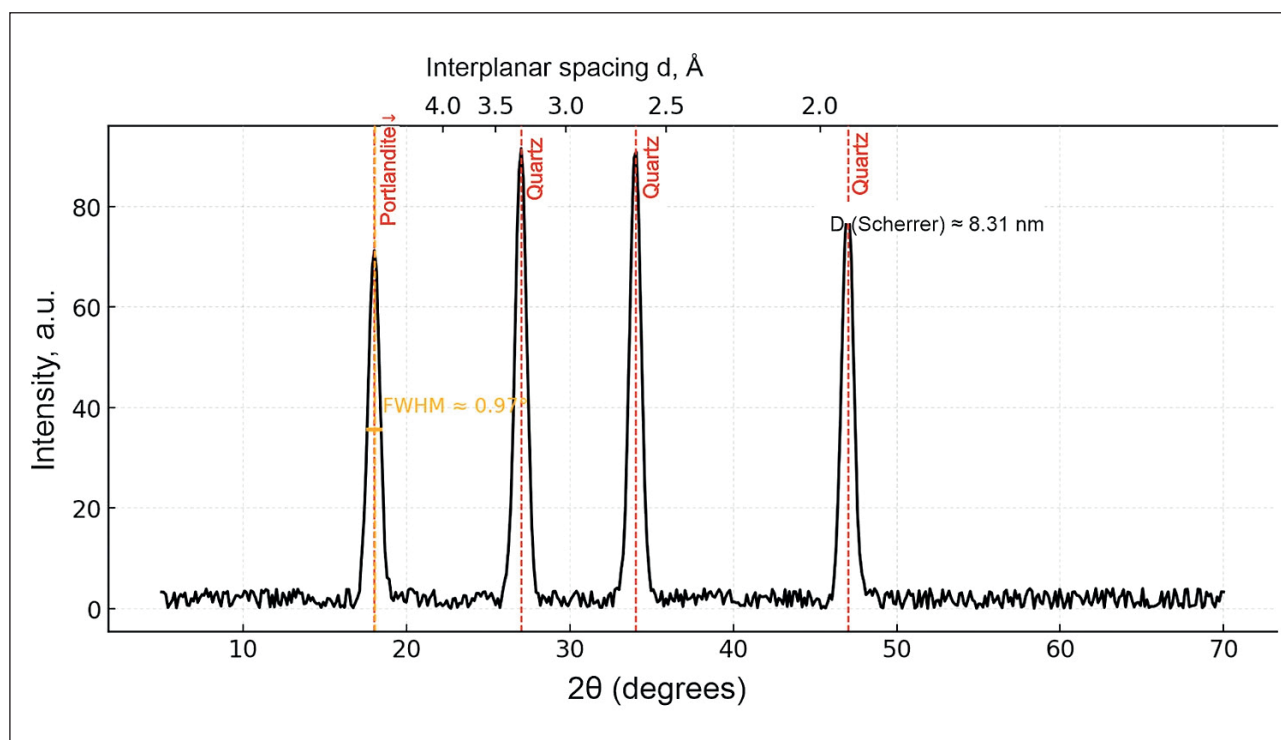


Fig. 11. X-ray diffraction (XRD) of polymer-modified mortar (PMM): peaks, FWHM, d-axis

in the regions of 12–13° and 31–33°, corresponding to hydrosulfoaluminates. A broad amorphous hump was observed between 25–35°, reflecting the formation of C–A–S–H gel. This confirms the predominance of amorphous phases, also evidenced by the low crystallinity index. The crystallite size calculated from the 31° peak using the Scherrer equation was 20–25 nm, indicating a nanostructured matrix. Such a structure provides geopolymers with high chemical resistance and long-term durability (Fig. 12).

Ultra-high-performance concrete (UHPC) showed almost complete absence of intense crystalline peaks, except for weak quartz reflections at 27°, 34°, and 47°. The main contribution to the diffractogram was a broad amorphous hump between 25–35°, associated with the formation of amorphous C–S–H gel. The crystallinity index was minimal, while the amorphous fraction was the highest among all materials. The analysis of the FWHM of the quartz peak at 27° indicated an average crystallite size of approximately 10–15 nm. This highly amorphous structure provides UHPC with exceptional mechanical properties, including a high elastic modulus and outstanding durability (Fig. 13).

A comparative analysis of all materials showed a consistent decrease in portlandite content, formation of amorphous phases, and reduction in crystallite size from the original concrete to PMM, geopolymers, and UHPC. The geopolymer system is characterized by the development of C–A–S–H gel and hydrosulfoaluminates, which enhance chemical stability, while UHPC

exhibits maximum amorphousness due to the dominance of C–S–H gel, directly linked to its ultra-high mechanical performance (Fig. 14).

Nanoindentation confirmed that UHPC possesses the highest local modulus values (40–50 GPa within the matrix), while geopolymers exhibited a range of 25–35 GPa (Table 6).

Comparative Analysis

Overall, UHPC provides the highest strength, structural density, and cavitation resistance, though it involves higher production costs. Geopolymer materials demonstrated exceptional resistance to sulfate attack and good mechanical performance. PMM can serve as a more economical solution for localized repair applications (Table 7).

Practical Significance

The results confirm that the rational selection of materials must account for both loading conditions and environmental exposure:

- UHPC – recommended for areas subjected to cavitation, high flow velocities, and impact loads;
- Geopolymer compositions – optimal for zones with high sulfate aggressiveness;
- PMM – suitable for cost-effective repair solutions and secondary structural elements.

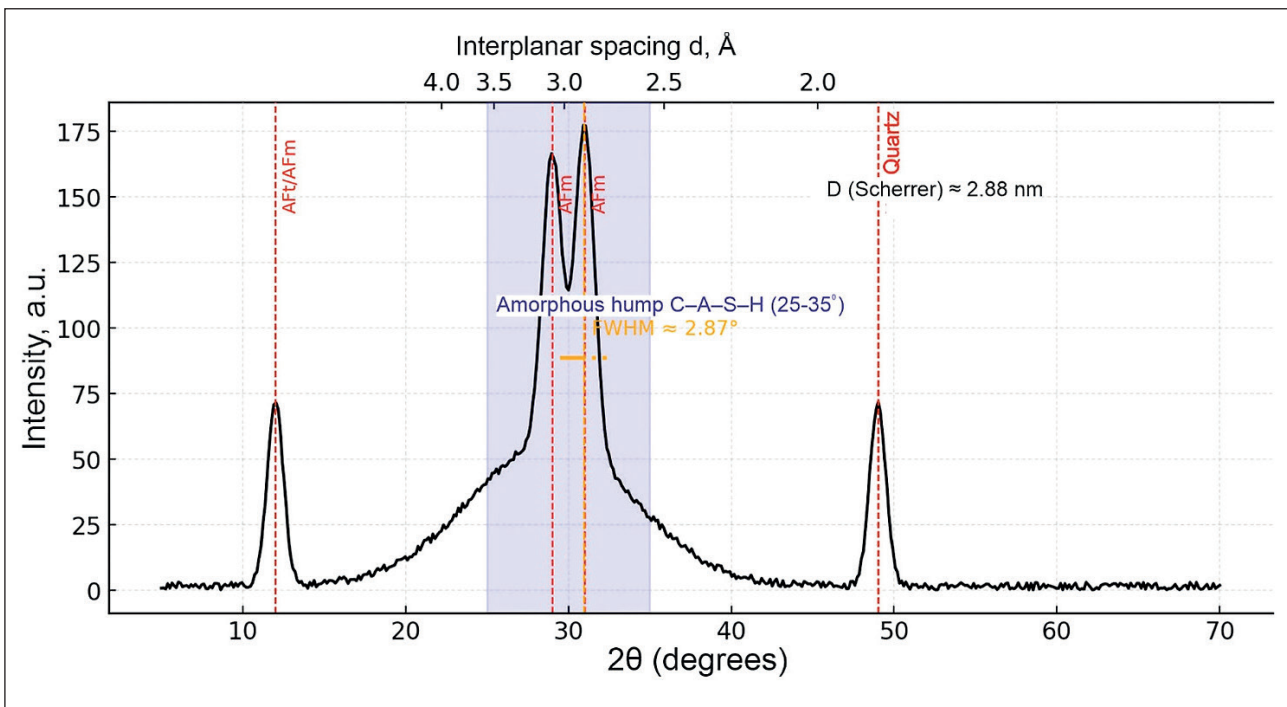


Fig. 12. X-ray diffraction (XRD) of geopolymer (GP): peaks, FWHM, d-axis

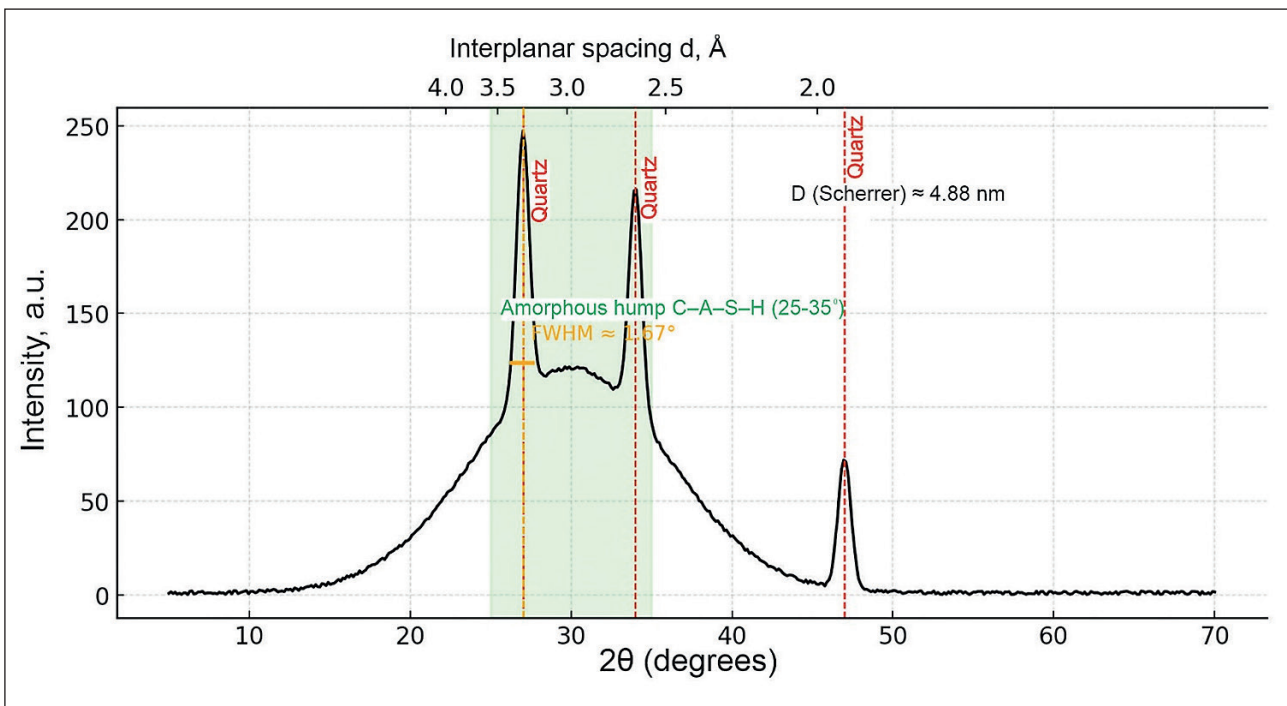


Fig. 13. X-ray diffraction (XRD) of ultra-high-performance concrete (UHPC): peaks, FWHM, d-axis

CONCLUSION

The conducted laboratory studies made it possible to comprehensively evaluate the properties of advanced materials for the restoration of concrete structures in

hydraulic engineering facilities. The data obtained demonstrate that the durability and serviceability of concrete elements are directly dependent on the microstructural characteristics and barrier performance of repair compositions.

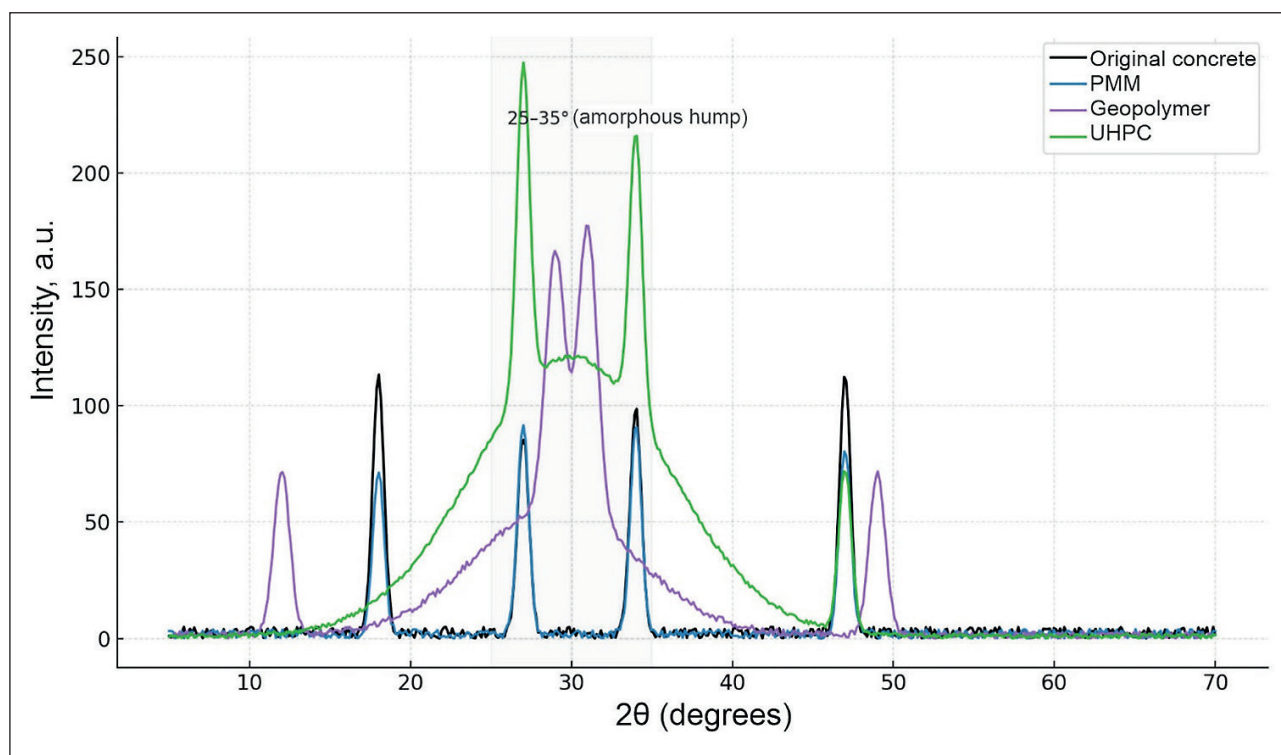


Fig. 14. Comparative XRD patterns of all materials

Table 6. Summary statistics of nanoindentation results

No.	System	E_{median} (GPa)	E_{IQR} (GPa)	H_{median} (GPa)	H_{IQR} (GPa)
1	Original concrete	23.0	~20–26	0.85	0.7–1.0
2	PMM	30.0	~28–32	1.0	0.8–1.2
3	Geopolymer	31.0	~28–35	1.05	0.9–1.3
4	UHPC	46.0	~44–48	1.4	1.2–1.6

Table 7. Comparison of key performance indicators of the systems

No.	Indicator	Original Concrete	PMM	Geopolymer	UHPC
1	f_c , MPa	34	58	72	150+
2	E , GPa	27	31	34	47
3	RCPT, C	5000	1500	800	300
4	Sorptivity, $\text{kg/m}^2 \cdot \text{h}^{0.5}$	0.25	0.12	0.06	0.03
5	Strength loss (F–T, %)	22	8	5	3
6	Expansion (sulfates, %)	0.30	0.16	0.04	0.06
7	Abrasion, $\text{g/m}^2 \cdot \text{h}$	40	21	10	6

1. The original concrete was characterized by high permeability (RCPT $\sim 5.2 \times 10^3$ C), pronounced porosity, and low frost and sulfate resistance. SEM confirmed the presence of large pores and microcracks, accelerating

degradation. These findings justify the necessity of applying modern repair materials.

2. PMM demonstrated a reduction in permeability to $\sim 1.5 \times 10^3$ C and an increase in adhesion strength up to

1.8 MPa but showed limited long-term durability under repeated loadings. Geopolymer compositions provided a low diffusion coefficient (5×10^{-12} m²/s), high sulfate resistance, and a fine, homogeneous pore structure confirmed by XRD and SEM. UHPC showed the best overall performance: permeability $< 0.3 \times 10^3$ C, adhesion 2.2 MPa, minimal strength loss under freeze–thaw cycles, and a high local elastic modulus (40–50 GPa). SEM revealed an extremely dense matrix with uniform fiber distribution.

3. XRD analysis confirmed a decrease in portlandite content in geopolymers and the formation of sulfate-resistant phases, as well as the predominance of amorphous C–S–H in UHPC. Nanoindentation verified the increase in local mechanical properties of UHPC and geopolymers compared to the original concrete.

4. UHPC is the most versatile and durable material for structures exposed to abrasive–cavitation wear and cyclic loading.

5. Geopolymer materials are recommended for sulfate-aggressive environments and limited-budget applications, where ecological performance is important.

6. PMM are justified for localized repairs and less-loaded zones.

Thus, this study has confirmed the feasibility of a comprehensive approach: defect diagnosis → selection of a rational material → laboratory verification → durability and life-cycle assessment. This approach provides an engineering basis for the design of repair and rehabilitation measures for hydraulic structures, considering the specific regional conditions.

REFERENCES

1. Moldamuratov Z.N., Ussenkulov Z.A., Yeskermessov Z.E., Shanshabayev N. A., Bapanova Z.Z., Nogaipekova M.T., Joldassov S.K. Experimental study of the effect of surfactants and water-cement ratio on abrasion resistance of hydraulic concretes. *Rasayan Journal of Chemistry*. 2023;16(3):1116–1126. <https://doi.org/10.31788/RJC.2023.1638391>
2. Zhakipbayev B.Ye., Zhakiyev N.K., Abdikadyr B.Z., Moldamuratov Zh.N., Abekov K.O. The Technology of Foam-Glass Building Materials for Heat-Insulating Purposes Using Amorphous-Silica Rocks. *ES Materials & Manufacturing*. 2025;27:1379. <https://dx.doi.org/10.30919/esmm1379>
3. Zhakipbayev B.Ye., Ismailova A.B., Tukhtamisheva A.Z., Seitkazinov O.D., Moldamuratov Zh.N. Energy efficiency and decarbonization of cement and foamed glass production through the use of natural active mineral additives (opoka and diatomite). *Nanotechnologies in Construction*. 2024;16(6):587–600. <https://doi.org/10.15828/2075-8545-2024-16-6-587-600>
4. Moldamuratov Z.N., Iglikov A.A., Sennikov M.N., Madaliyeva E.B., Turalina M.T. Irrigation canal lining using shotcrete with additives. *Nanotechnologies in Construction*. 2022;14(3):227–240. <https://doi.org/10.15828/2075-8545-2022-14-3-227-240>
5. Moldamuratov Zh.N., Ismailova A.B., Tukhtamisheva A.Z., Yeskermessov Zh.E., Rakhimov M.A. Experimental study of asphalt concrete as the optimal material for lining irrigation canals. *Nanotechnologies in Construction*. 2024;16(2):125–139. <https://doi.org/10.15828/2075-8545-2024-16-2-125-139>
6. Suleimenov Z.T., Sagyndykov A.A., Moldamuratov Z.N., Bayaliyeva G.M., Alimbayeva Z.B. High-strength wall ceramics based on phosphorus slag and bentonite clay. *Nanotechnologies in Construction*. 2022;14(1):11–17. <https://doi.org/10.15828/2075-8545-2022-14-1-11-17>
7. Moldamuratov Z.N., Imambayeva R.S., Imambaev N.S., Iglikov A.A., Tattibayev S.Z. Polymer concrete production technology with improved characteristics based on furfural for use in hydraulic engineering construction. *Nanotechnologies in Construction*. 2022;14(4):306–318. <https://doi.org/10.15828/2075-8545-2022-14-4-306-318>
8. Kabdushev A.A., Agzamov F.A., Manapbayev B.Z., Moldamuratov Z.N. Microstructural analysis of strain-resistant cement designed for well construction. *Nanotechnologies in Construction*. 2023;15(6):564–573. <https://doi.org/10.15828/2075-8545-2023-15-6-564-573>
9. Jumadilova S.Zh., Khomyakov V.A., Kenebayeva A.K., Moldamuratov Zh.N. The use of geosynthetic materials to increase the bearing capacity of soil cushions. *Nanotechnologies in Construction*. 2024;16(4):342–354. <https://doi.org/10.15828/2075-8545-2024-16-4-342-354>
10. Kattakulov F., Muslimov T., Khusainov A., Sharopov S., Vokhidov O., Sultanov S. Water resource saving in irrigation networks through improving the efficiency of reinforced concrete coatings. In *IOP Conference Series: Materials Science and Engineering*. 2020. <https://doi.org/10.1088/1757-899X/883/1/012053>
11. Baev O.A., Talalaeva V.F. Design and technological solutions for irrigation canal coating formation and resurfacing. *Land Reclamation and Hydraulic Engineering*. 2022;(2). <https://doi.org/10.31774/2712-9357-2022-12-2-177-191>

12. Okhapkin G.V. Approaches to a Digital Transformation of the Choice of Technical Solutions for the Restoration of the Concrete Bulk Structure of Hydraulic Engineering Structures. *Power Technology and Engineering*. 2023;57(3):394–398. <https://doi.org/10.1007/s10749-023-01674-x>
13. Choi D., Hong K., Ochirbud M., Meiramov D., Sukontaskuul P. Mechanical Properties of Ultra-High-Performance Concrete (UHPC) and Ultra-High-Performance Fiber-Reinforced Concrete (UHPFRC) with Recycled Sand. *International Journal of Concrete Structures and Materials*. 2023;17(1):128. <https://doi.org/10.1186/s40069-023-00631-2>
14. Rubin O., et al. Strengthening of Reinforced Concrete Hydraulic Structures using external carbon ribbons. *Buildings*. 2024; 14(12): 3739. <https://doi.org/10.3390/buildings14123739>
15. Tan B., Qu L., Xia Y., Yang X., Su B., Wu J., Xiao M. Experimental Study on Improving the Impermeability of Concrete under High-Pressure Water Environments Using a Polymer Coating. *Applied Sciences*. 2024;14(18):8507. <https://doi.org/10.3390/app14188507>
16. Kravanja G., et al. A Comprehensive Review of the Advances, Manufacturing, and Applications of Ultra-High-Performance Concrete (UHPC). *Buildings*. 2024;14(2):382. <https://doi.org/10.3390/buildings14020382>
17. Saladi N., et al. Assessing durability properties of ultra-high-performance concrete. *Materials and Structures*, 2023. <https://doi.org/10.1617/s11527-023-02244-3>
18. Xie M., et al. Preparation Technology and Experimental Study of Fast UHPC Repair Materials. *Buildings*. 2024;14(7):2124. <https://doi.org/10.3390/buildings14072124>
19. Okhapkin G.V. Analysis of Approaches to Selecting Repair Materials for Restoration of Hydro-Technical Facilities. *Gidrotekhnicheskoe Stroitelstvo / Hydrotechnical Construction*. 2022. <https://doi.org/10.1007/s10749-023-01468-1>
20. Wang Z., Liu Y., et al. Review on Repair Technologies for Underwater Concrete Structures. *Water*. 2024;17(1):35. <https://doi.org/10.3390/w17010035>
21. Zheng H., et al. Performance study of a tough and non-dispersible dual epoxy modified cement paste (SDEP). *Construction and Building Materials*. 2025. <https://doi.org/10.1016/j.conbuildmat.2025.128214>
22. Bibina O.E., Okhapkin G.B. Some Approaches to the Repair of Cracks in the Concrete of Hydraulic Structures. *Power Technology and Engineering*. 2023;57:551–556. <https://doi.org/10.1007/s10749-024-01699-w>
23. Rubin O., Kozlov D., et al. Strengthening of Reinforced Concrete Hydraulic Structures with External Reinforcement System Made of Carbon Fiber-Based Composite Materials. *Buildings*. 2024;14(12):3739. <https://doi.org/10.3390/buildings14123739>
24. Omoregie A.I., et al. Bio-Based Solutions for Concrete Infrastructure: A Review. *Buildings*. 2025;15(7):1052. <https://doi.org/10.3390/buildings15071052>
25. He Y., et al. Effect of seawater dry-wet cycling on the durability of repair materials. *Journal (Tandfonline)*. 2024. <https://doi.org/10.1080/21650373.2023.2279288>
26. Krelani V., Ahmeti M., Kryeziu D. Increased Durability of Concrete Structures Under Severe Conditions Using Crystalline Admixtures. *Buildings*. 2025;15(3):352. <https://doi.org/10.3390/buildings15030352>
27. Wang S., et al. Research on improving the durability performance of damaged concrete by UHPC repair. *Engineering Research & Technology (Wiley)*. 2024. <https://doi.org/10.1002/eng2.12780>
28. Affandi Mohd Zahid MZ, et al. Review on the potential of waste materials in developing green UHPC for rehabilitation works. *Materials / Sustainable Materials Journal*. 2025. <https://doi.org/10.1007/s44290-025-00282-0>
29. Provis J.L. Durability and material failures in concrete: recognizing complexity when planning repairs. *Nature Materials / similar*. 2024. <https://doi.org/10.1038/s44172-024-00172-w>
30. Rakhimov, M.A., Aubakirova, Z.A., Aldungarova, A.K., de Navascués, I.M.P., Moldamuratov, Z.N. Optimization of a sustainable composition of fine-grained concrete for 3D-printing with partial substitution of sand with fly ash and slag waste. *Nanotechnologies in Construction*. 2025;17(3):296–306. <https://doi.org/10.15828/2075-8545-2025-17-3-296-306>

ADDITIONAL INFORMATION

The authors declare that generative artificial intelligence technologies and technologies based on artificial intelligence were not used in the preparation of the article.

INFORMATION ABOUT THE AUTHORS

Karlygash I. Ilyassova – M.S., Assistant Professor, School of Engineering, International Educational Corporation, Almaty, Kazakhstan, k.ilyasova@kazgasa.kz, <https://orcid.org/0000-0002-6994-4806>

Zhangazy N. Moldamuratov – PhD, Research Professor, School of Construction, International Educational Corporation, Almaty, Kazakhstan, zhanga_m_n@mail.ru, <https://orcid.org/0000-0002-4573-1179>

Orazaly D. Seitkazinov – Cand. Sci. (Eng.), Associate Professor, School of Construction, International Educational Corporation, Almaty, Kazakhstan, oseitkazinov@mail.ru, <https://orcid.org/0000-0002-4854-3747>

Guldana S. Abiyeva – Cand. Sci. (Eng.), Associate Professor, School of Construction, International Educational Corporation, Almaty, Kazakhstan, g.abiyeva@kazgasa.kz, <https://orcid.org/0000-0002-0101-2252>

Ainur Z. Tukhtamisheva – PhD, Associate Professor, School of Engineering, International Educational Corporation, Almaty, Kazakhstan, aynurjan_kz@mail.ru, <https://orcid.org/0000-0001-8945-3783>

Manizha Paktin – M.S., Assistant Professor, School of Construction, International Educational Corporation, Almaty, Kazakhstan, m.paktin@kazgasa.kz, <https://orcid.org/0009-0006-7348-2372>

CONTRIBUTION OF THE AUTHORS

Karlygash I. Ilyassova – conducted experimental studies, prepared mixtures, performed strength and expansion tests, carried out preliminary data analysis, and participated in the preparation of illustrative materials.

Zhangazy N. Moldamuratov – provided scientific supervision of the project, developed the overall structure of the article, and ensured quality control at all stages of the research.

Orazaly D. Seitkazinov – performed scientific editing and text refinement, formulated conclusions, and developed practical recommendations.

Guldana S. Abiyeva – selected and justified the composition of alkaline activators, analyzed the influence of curing conditions, contributed to the preparation of the “Materials and Methods” section, and compiled the abstract and keywords.

Ainur Z. Tukhtamisheva – provided methodological support, formulated the research hypothesis, ensured the correctness of the experimental design, and participated in writing and editing the article text.

Manizha Paktin – contributed to defining the research aim and objectives, wrote the introduction and conclusion, and substantiated the practical significance of the study.

The authors declare no conflicts of interest.

The article was submitted 26.10.2025; approved after reviewing 04.12.2025; accepted for publication 07.12.2025.